Selected Methods of Image Analysis in Optical Coherence Tomography

Robert Koprowski and Zygmunt Wróbel

University of Silesia, Faculty of Computer Science and Materials Science
Institute of Computer Science, Department of Biomedical Computer Systems
Poland

1. Introduction

OCT is a new technique of picturing that uses uninvasional and contactless optical method based on interferometry of partially compact light for receiving sections images of human eyes in vivo. It allows picturing structural changes caused by eyes diseases, mapping thickness of retina and analyses shield of optical nerve and coats of nerve fibers. OCT has been developed since 1995 when it was initiated by measurement of intraocular distance by A.F. Frechera (Fercher el at., 1995) in years 2002-2004 the quick growth of quality and speed of eye picturing acquisition was observed but particularly in 2003 linear picturing and 2004 fast picturing with high resolution –Fig. 1. (Leitgeb el at., 2004; Ozcan el at., 2007; Bauma B. E. & Tearney, 2002).
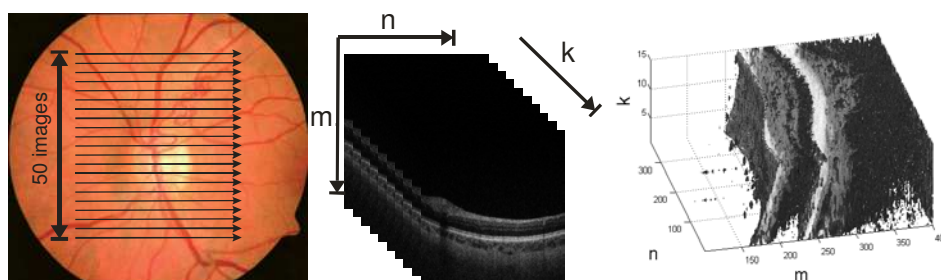

Fig. 1. The comparison of normal optic nerve head images with differential optical coherence tomography (OCT) technologies M×N×K=740×800×50

In work have been won input images L_{GRAY} in number near 1000 from optical tomograph SOCT Copernicus in the following parameters: wave length of light source: 840nm, width of spectrum: 50nm, pivotal resolution width (longitudinal): 6μm, traverse resolution: 12-18 μm of tomograph window: 2mm, speed of measurement: 25 000 scans in k pivot per second, maximum width of scanning: 10mm, maximum number of punctual scans in k pivot falling to n pivot: 10 500, become write down in gray levels about resolution M×N×K=740×800×50 where for each pixel falls to 8 bits.

The next part of considerations will be concerned with methods of analysis and processing of images automatically appointing layers borders visible on fig. 2 like: RPE – Retinal

Pigment Epithelium, OPL – Outer plexiform layer, IS/OS – Boundary between the inner and outer segments of the photoreceptors.
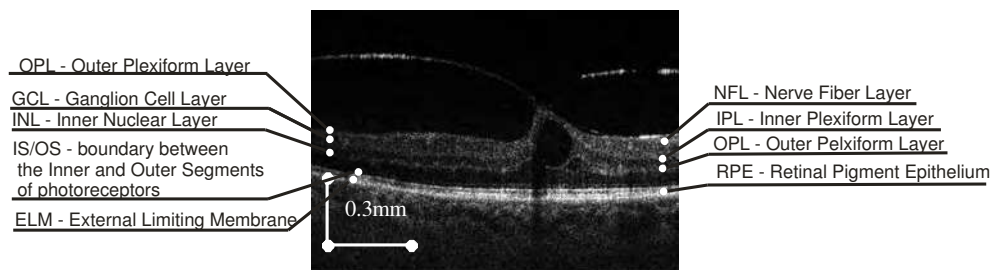

Fig. 2. Section scheme of individual layers along with marked characteristic gauged areas – image taken from SOCT Copernicus.

These considerations will be concerned with analysis of images sequences that have been already archived. Therefore, the possibilities of interference with the OCT device's apparatus will not be considered for increasing range of brightness level. Data from images sequence will not be taken into account, either - each image is analyzed independently. The source of acquiring given images assigned for analyses described by algorithms is free, i.e. any OCT device which allows to receive 2D image about minimum resolution 300×400 pixels.

The need of thickness analysis of individual layers RPE, IS/OS, NFL or OPL results from necessity of quantitative assessment but not qualitative, e.g. disease progression or efficiency of therapy, e.g. diabetes or Birdshot Chorioretinopathy.

Four methods of individual visible layers analyses will be discussed on Fig. 2 namely:

- Method of modified active contour – ACM. This method is based on basic information acquired from image like for example: the lightest RPE layer which will be identified in first period and on its base the remaining layers analysis will be carried out as OPL or IS/OS method of modified active contour for implemented line.

- The wandering small part method in discovering Canny edge - CCA. This method relies on preliminary edge detection using Canny detector and next continuity of lines correction on ends and conducting their connection with remaining ones (Canny, 1986; Koprowski & Wróbel, 2008).

- Random method of contour analysis – RAC. Points that start marking the edges are chosen at random during the preliminary image period, next the correction of their numbers is carried out in order for the remaining numbers, that come up to certain expectations, to become the first points of the lines appointed with the wandering small part method (Koprowski & Wróbel, 2009).

- Method based on hierarchic approach - HAC . There is preliminary identification of main layers like OPL or RPE on the smallest resolution and then the remaining layers are identified like IS/OS and the layers reconnaissance accuracy is gradually improved OPL and RPE (Koprowski & Wróbel, 2009).

2. Present state of knowledge - results acquired with known algorithms

Among results acquired with known algorithms there is in this chapter the description of the results:

- Acquired by other authors
- Acquired by authors of this work which have not brought satisfactory results in this application.

2.1 Results acquired for algorithms processed by authors not bringing desired results for OCT images

Among these results there have been methods which have not given satisfactory results as:

1. Method using Hough transform (Gonzalez & Woods, 1992). This method in this case did not give satisfactory results because the wanted layers on OCT image can change thickness and in general case can not be continuous. Additionally, the radius of curvature describing border of layers can be changed in wide ranges (Koprowski & Wróbel, 2009). It happens for example in shield of optical nerve (Costa el at., 2006) where individual OPL layers , RPE or IS/OS they are much worse visible (Klinder el at., 2009). Certain improvement of this method would be area analysis in which individual areas (with given width) would be brought closer by the lines. However, in this case emerges their mutual connections problem and problem of computational complexity.
2. Method of active contour in its typical version also does not produce desired results (Liang el at., 2006). At automatic selection of starting points using for example, method of Canny contour discovering or Gabor's filters (Gonzalez & Woods, 1992) only borders between the layers with the greatest contrast are discovered – RPE. In other cases, for the others layers, the method does not produce the expected results unless it is applied interactively with the user. Because the considerations in this work are applied only to fully automatic methods, the above method cannot be taken into account because of the mentioned interaction with the user. The method after the modifications introduced by the authors will be presented later in the algorithm ACM and CCA.
3. Method of texture analysis. In this case individual OPL layers, RPE or IS/OS are similar in case of texture which almost by definition disqualifies the described method. Despite this fact, the methods of texture analysis can be successfully used for emitting the wanted object from background (vitreous body). For example, for other type of images the methods have been successfully used in segmentation (Farsiu el at., 2008).
4. Also, methods of extended objects analyses (Koprowski el at., 2005) do not find application here because of the possibility of great size change in both the very object and its thickness and also the possibility of the object's division into two or more parts.

Methods suggested below in the work and processed by the authors (Koprowski el at., 2005, 2008, 2009) are a modification of the already mentioned known methods of analyses and processing of images and they are also new algorithms protected by copyright.

2.2 Results acquired by other authors

According to the best of author's knowledge there are no known algorithms analyses of eyes retina taking into account discovering the mentioned borders OPL, RPE or IS/OS including shield of optical nerve. Approaches suggested and introduced in (Chinn el at., 1997) or (Drexler el at., 2003) work only for typical cases in which the degree of pathology is insignificantly small. Applications used and enclosed for OCT device for example Copernicus also do not work successfully. In case of greater pathology, layers identified automatically are not continuous or they are not identified in a correct manner. The erroneus action that occurs often is incorrect connection of the identified layers and

erroneous identifying of optical nerve shield. Additionally, the realized applications added to such a device like Copernicus or Stratus they are protected by copyright and rigorous form of algorithm is not rendered accessible outside. It results in the inability to estimate quantitatively the results and their accuracy in comparison with the author approaches suggested in this work.

Despite it, there is a whole big group of methods working correctly for simple cases where in OCT images there are well identified (with sufficient contrast) individual layers. They are the methods processed in LabVieW or in C++ (for example Bauma B. E. & Tearney, 2002) the processed results were also published in user manual Copernicus (Optopol) or in one of the chapters (Barry, 205). In this last position of literature (Farsiu el at., 2008) one of the few applications that analize individually further discussed OPL or RPE layers completely automatically is presented. It seems that OCT image analysis of eye is similar to the analysis of skin, or even coat material of a tennis ball (Thrane, 2001) however, the specificity of approach lies in variability in thickness of layers, individual variability of individual cases. In such cases of thickness changes of individual RPE, IS/OS, NFL or OPL layers, their mutual positions can be so big that typical algorithms work incorrectly. Obviously, there is coordinately a whole remaining group of methods interacting with user in which the user indicates representative or marks of segmentation area, giving off of layer and the implemented algorithm using, for example, the method of area expansion segmentates the marked area (Klinder el at., 2009), or fractal analisys. Algorithms for which correct results were acquired even for images of big radius of pathology distortion that work fully automatically are presented in next chapters in the form of block schemes. Detailed description of individual steps of discussed algorithms and their property like for example sensitivity to parameters change is discussed in given publications (Koprowski el at., 2005, 2008, 2009).

On this basis, taking into account also medical premises and taken attempts introduced below, four algorithms of analyses and processing of images of eye retina layers OCT were suggested.

3. The description of the suggested and compared algorithms

The algorithms presented below are both, known from the literature and modified by the authors and also new ones. Individual layers are marked in Cartesian coordinate match like RPE-y_{RPE}, IS/OS – $y_{IS/OS}$ layer. To avoid the conflict in designation, in chosen cases overhead index indicating algorithm type (ACM, CCA, RAC or HAC) – for example $y_{RPE}^{(CCA)}$ was added.

3.1 Preliminary processing of image

Preliminary processing of image is common for all discussed methods ACM (Koprowski & Wróbel, 2009), CCA -(Koprowski & Wróbel, 2008), RAC (Koprowski el at., 2005) or HAC (Koprowski & Wróbel, 2009). Preliminary algorithms of processing of images include filtration with median filter of square mask sized about 21×21 for elimination of hum and slight artefacts introduced by measuring match in the course of acquisition of image. Selection of size of mask has been carried arbitrarily on base of image resolution M×N=740×800 and width of interests layers(OPL, RPE or IS/OS). Obviously, it must be mentioned here that there are many others methods belonging to filtration in preliminary

processing of image like for example adaptation filters, spatially adaptive wavelet filter (Adler et al., 2004; Gnanadurai & Sadasivam, 2005) or fuzzy-based wavelet.

The second element of processing of preliminary image was normalization from minimum-maximum partition of image pixels brightness for full partition from 0 for 1. This procedure is aimed at the expansion of pixel brightness range for image on which the quality of visible object is degraded for different reasons.

So transformed images L_{MED} (after filtration of median filter and normalization) were subjected to analysis with available algorithms and algorithms suggested by authors (ACM, CCA, RAC, HAC).

3.2 Description of ACM algorithm

The ACM method - active modified contour, it is based on basic information acquired from image like for example the plainest RPE layer which will be identified in the first period and on its base the analysis of the remaining layers like OPL or IS/OS will be carried out (Akiba et al., 2003; Choma el at., 2003). The picture 3 presents structure of unit algorithm (block scheme) in which chosen blocks (layer analysis OPL, IS/OS, ELM) can work independently.
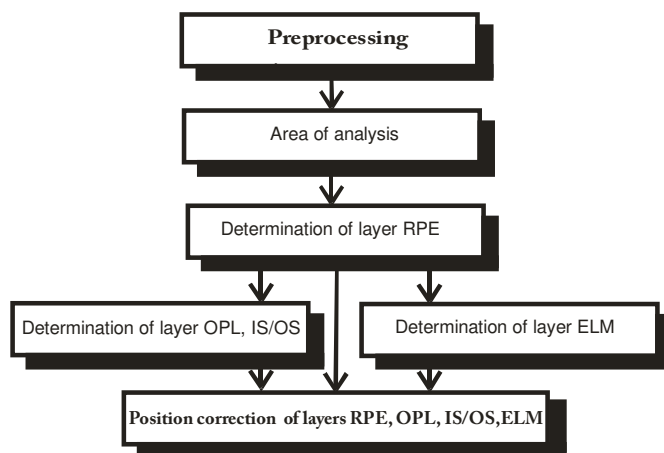
Fig. 3. Block scheme of algorithm

The block scheme introduced in picture 3 divides the work of the whole ACM algorithm into four phases::

- Preliminary processing – filtration with median filter and normalization were described in the former subchapter.
- Appointing of RPE layer site and next using modified active contour method assigning remaining OPL or IS/OS layers.
- Appointment of external border of ELM retina site.
- Correction of the received layers in relation to the   area of analysis - taking into account quality of areas of introduced objects.

After preliminary process of image processing (filtration and normalization receiving L_{MED}) L_{GRAY} image analysis was started by analyzing the place of maximum for next columns of images matrixes. If we mark lines and columns of the image matrixes by m and n new $L_{BIN}^{(ACM)}$ image includes value "1" in places where pixels are brighter in given column by

90% for this column maximum taking a stand brightness. In the remaining places there is value "0". On this base calculating of the center sites of longest section for each image column $L_{BIN}^{(ACM)}$ receiving course y_R was carried out (Fig. 2).
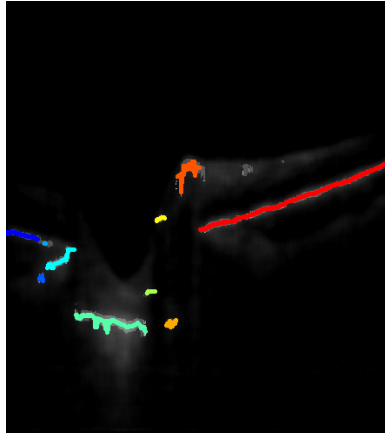

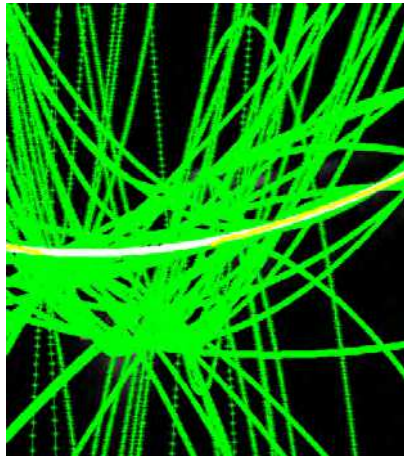Fig. 4. The sum of $L_{BIN}^{(ACM)}$ image in 50% weight and 50% L_{MED} and drawn y_R course (y_{RS}),

Fig. 5. Functions of 3th row $y_{RS}(k_1,k_2)$ for any possible couples of concentrations

Course of y_R function is further subjected to the operation of concentrations analyses by k-means method acquiring $y_{RS}^{(k)}$ for each k-concentration. Next the operation of approxymation through polynomial of 3 row ($y_{RS}^{(k1,k2)}$) of each couple $y_{RS}^{(k1)}$ and $y_{RS}^{(k2)}$ for $k_1 \neq k_2$ is performed. All polynomial functions $y_{RS}^{(k1,k2)}$ received for all possible pairs of concentration (k_1, k_2) are shown in Fig. 2-3. For each function y_R a number of points is appointed contained in partition ±15 pixels. Next the pair (k_1,k_2) is appointed for which number of point contained in partition ±15 pixels is maximum at chosen $y_{RS}^{(k1^*,k2^*)}$ in simplification further called y_{RPE} function. Result is shown in Fig. 2-3 by white line (course of $y_{RPE}^{(ACM)}$). ELM and IS/OS borders were appointed on the basis of course $y_{RPE}^{(ACM)}$.

Algorithms in both cases were very approximated for each other and they concerned in biggest fragment method of modified active contour (exact differences between suggested method and classic method of active contour is shown in Gonzalez & Woods 1992). According to the introduced visual scheme in Fig. 5 values of medians in areas over and below of analysis pixel in blocks about sizes $p_{yu} \times (p_{xl}+p_{xp}+1)$ for method of active contour are appointed.

Next the value of their remainder is calculated and written down in matrix ΔS in following form:

$$
\Delta S = \begin{array}{c} \cdots \\ 4 \\ 3 \\ 2 \\ 1 \\ 0 \\ -1 \\ -2 \\ -3 \\ -4 \\ \cdots \end{array} \left\{ \begin{array}{cccc} & & \cdots & \\ \Delta_{S,4,1} & \Delta_{S,4,2} & \Delta_{S,4,3} & \Delta_{S,4,4} \\ \Delta_{S,3,1} & \Delta_{S,3,2} & \Delta_{S,3,3} & \Delta_{S,3,4} \\ \Delta_{S,2,1} & \Delta_{S,2,2} & \Delta_{S,2,3} & \Delta_{S,2,4} \\ \Delta_{S,1,1} & \Delta_{S,1,2} & \Delta_{S,1,3} & \Delta_{S,1,4} \\ \Delta_{S,0,1} & \Delta_{S,0,2} & \Delta_{S,0,3} & \Delta_{S,0,4} \quad \cdots \\ \Delta_{S,-1,1} & \Delta_{S,-1,2} & \Delta_{S,-1,3} & \Delta_{S,-1,4} \\ \Delta_{S,-2,1} & \Delta_{S,-2,2} & \Delta_{S,-2,3} & \Delta_{S,-2,4} \\ \Delta_{S,-3,1} & \Delta_{S,-3,2} & \Delta_{S,-3,3} & \Delta_{S,-3,4} \\ \Delta_{S,-4,1} & \Delta_{S,-4,2} & \Delta_{S,-4,3} & \Delta_{S,-4,4} \\ & & \cdots & \end{array} \right.
\tag{1}
$$

Where ΔS=med(Lu)-med(Ld) for Lu and Ld that are areas of the size properly $p_{yu} \times (p_{xl}+p_{xp}+1)$ and $p_{yd} \times (p_{xl}+p_{xp}+1)$ and

p_{yu} - value of Lu line,
p_{yd} - value of Ld line,
p_u - partition of relocation pixel and areas Lu i Ld for top,
p_d - partition of relocation pixel and areas Lu i Ld to bottom,
p_{xl} - number of column on the left of the analyzed pixel,
p_{xp} - number of column on the right of the analyzed pixel,
p_{ly} - distance in pivot oy respect $y_{RPE}^{(ACM)}$
p_{xud} - distance between neighbor pixels in pivot oy,
med – medians.

After creating ΔS matrix about size $(p_u+p_d+1) \times N$ sorting is performed for next columns begining from biggest values of remainders between Lu and Ld areas. Next the analysis of individual values for the following columns so that the pxud remainder does not surpass the assumed level is performed. For 1000 pieces of test images this value was established at the level of 2. The remaining parameters like pyu and pyd influence the sensitivity of the method and p_u and p_d are the range of searching possible pixels sites. By increasing p_{yu} and pyd values, time of calculations is increased. Searching for the new values of sites points of $y_{IS/OS}^{(ACM)}$ layer is started from course $y_{RPE}^{(ACM)}$. Points of initial $y_{IS/OS}^{(ACM)}$ layer emerge from slip by pIy in attitude of $y_{RPE}^{(ACM)}$ course.

New sites are appointed in partition from $y_{IS/OS}^{(ACM)}-p_{yu}$ to $y_{IS/OS}^{(ACM)}+p_{yd}$.

The received $y_{IS/OS}^{(ACM)}$, $y_{RPE}^{(ACM)}$, $y_{ELM}^{(ACM)}$ course (layers) must additionally grant the following conditions from premises subsequent of eye structure (these conditions will be served in Cartesian coordinate match) (Hausler & Lindner, 1998):

- $y_{RPE}^{(ACM)} < y_{IS/OS}^{(ACM)} < y_{ELM}^{(ACM)}$ for each x,
- $y_{ELM}^{(ACM)} - y_{RPE}^{(ACM)} \approx 0.1$ mm –being the initial value starting work of active contour method (Ko el at., 2005),
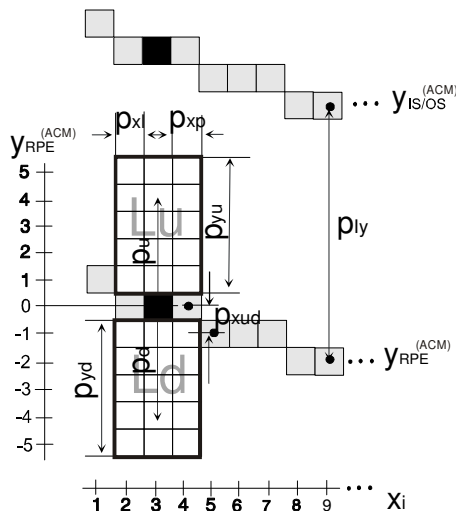- $y_{ELM}^{(ACM)} - y_{IS/OS}^{(ACM)} \approx$ od 0 do 1 mm for different x (Yun el at., 2004).

Fig. 6. Scheme of visual values scaling difference of brightness method

Appling this restriction, correct results for automatic achieved RPE, IS/OS or ELM layer finding has been achieved (Fig. 7).
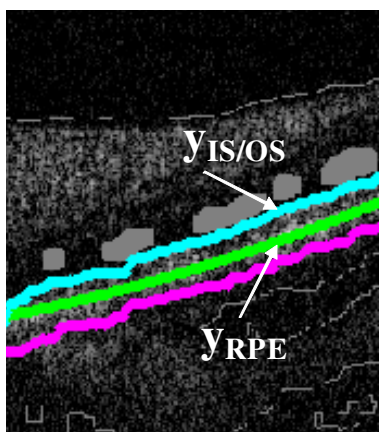
Fig. 7. Accommodation of function course $y_{IS/OS}^{(ACM)}$ and $y_{RPE}^{(ACM)}$.

3.3 Description of CCA algorithm

Method of small part wandering about in discovering Canny edge – CCA relies on preliminary detection of edge using Canny detector and next corrections of lines continuity on ends and performing the connection with the remaining ones– Fig. 8.
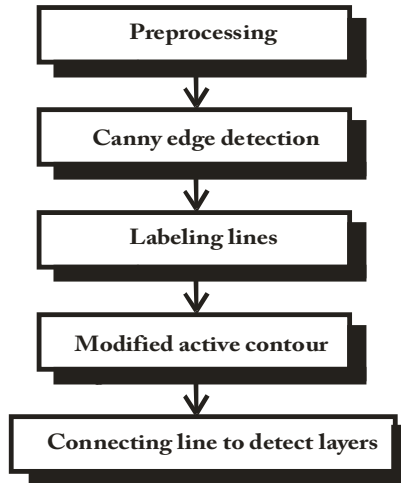
Fig. 8. Block scheme of CCA algorithm

The first period of the used CCA method is discovering edge with assistance of Canny method (Canny, 1986) on L_{MED} image. For so emerged binary $L_{BIN}^{(CCA)}$ the operation of labeling was conducted where each concentration (about value "1") owns label et=1,2,...,Et-1,Et. Next, for each label et labeling is conducted giving each concentration (line) label. Received image $L_{IND}^{(CCA)}$ is shown in pseudocolors on Fig. 7.
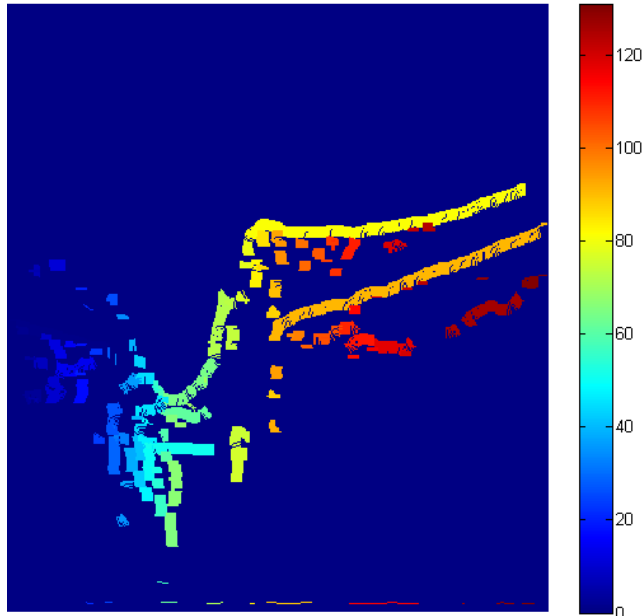

Fig. 9. $L_{IND}^{(CCA)}$ Image in pseudocolors (label Et=131)

Fig. 9 shows values of labels for the next line of $L_{IND}^{(CCA)}$ image. Each continuous line of edge visible on $L_{IND}^{(CCA)}$ image (Fig. 9) for labels $e_t=1,2,...,E_t-1,E_t$ has been transformed for form $k=1,2,3,…,K-1,K$ points $(x_{et,k}\ y_{et,k})$ in Cartesian match of coordinates. Method of modified active contour has been employed for each "stretch" of edge in both directions. For this purpose for two first pairs of coordinates of first edge $(x_{1,1},y_{1,1})$ and $(x_{1,2},y_{1,2})$ and two last ones $(x_{1,K-1},y_{1,K-1})$ and $(x_{1,K},y_{1,K})$ a straight line has been appointed going through these points, that is according to visual drawing below (Fig. 10):
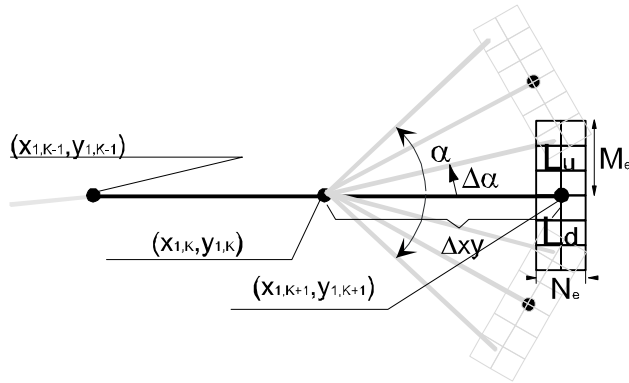
Fig. 10. Graphic interpretation of modified active contour method for appointment of next point beginning from points positions $(x_{1,K-1},y_{1,K-1})$ and $(x_{1,K},y_{1,K})$ for establishing new point (pixel) $(x_{1,K+1},y_{1,K+1})$. For simplification angle of depression of final points of edges was established at $\beta=0^o$.
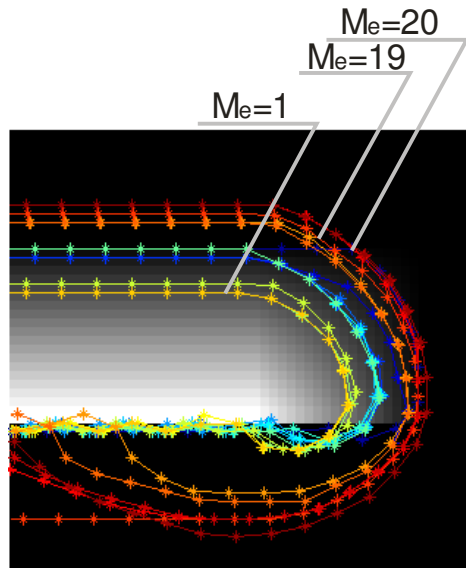

Fig. 11. Artificial image and fragment of modified active contour operation for $\alpha=40$, $\Delta\alpha=1$, $\Delta xy=N_e=4$, M_e changed in range (1,20)

Fig. 11 presents the ideas of method of active contour where beginning from points position $(x_{1,K-1}, y_{1,K-1})$ and $(x_{1,K}, y_{1,K})$ straight line going through them is established with an angle of depression β_1 and in distance Δxy appointing of the position of new point $(x_{1,K+1}, y_{1,K+1})$ for different potential positions (in angle partition $\beta_1(1) \pm \alpha$ through $\Delta\alpha$). The choice of proper position of contour point acquired through adding next points for existing edge is acquired on base of analyses of average values from areas Lu and Ld about size $M_e \times N_e$ (Fig. 3-8). α angle for which the best adjustment for the analyzed point $(x_{1,K+1}, y_{1,K+1})$ exists is the one for which the remainder in average values between areas Lu and Ld is the biggest.

As it happens, the suggested method of modified active contour has very curious properties. The parameters of this algorithm are as follows:

α - Angle in which range the best adjusting for the given criterion is searched,

$\Delta\alpha$ - Accuracy with which we search for the best adjusting,

Δxy - the distance between the present and the next searched point of active contour $(x_{1,K+1}, y_{1,K+1})$, $(x_{1,K+2}, y_{1,K+2})$ and so on,

Me - Height of analyzed Lu and Ld area

Ne - Width of analyzed Lu and Ld area

On the base of the above-mentioned findings and realized measurements (Koprowski & Wróbel, 2009) values of parameters of active contour on $\alpha=45$, $\Delta\alpha=1$, $\Delta xy=1$, Me=11, Ne=11 were established. Iterations for individual et edges of active contour method have been interrupted, then if one of the following situations happened:

The possible number of iterations has been surpassed - established arbitrary for 1000,

For this point the condition of remainder in average values between areas Lu and Ld has not been granted

At least two points own the same coordinates - it precludes to looping of algorithm.

For parameters established this way, the results have been acquired that are presented below Fig. 10, Fig. 11).
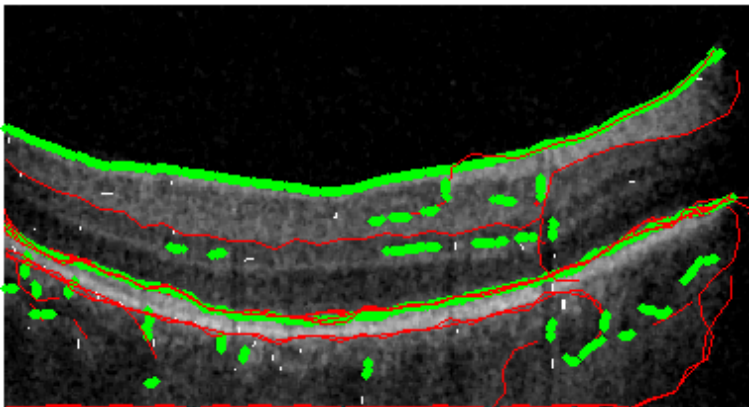

Fig. 12. Operation of modified active contour on real image for $\alpha=40$, $\Delta\alpha=1$, $\Delta xy=Ne=11$, Me =10. The green line marks the contour acquired with Canny method, the red line marks next points of active contour method.

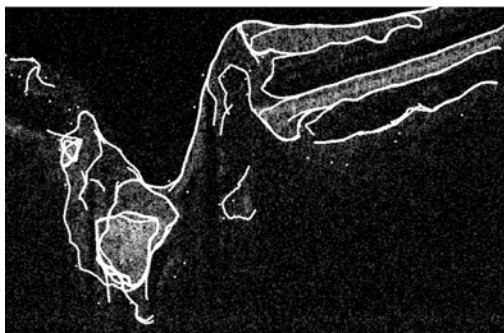Fig. 13. Operation of modified active contour after the described correction on real image for α=40, Δα=1, Δxy=Ne=11, Me =11

As shown on drawings above (Fig. 10, Fig. 11) the suggested method discovers correctly individual layers on OCT image of an eye.

3.4 Random method of contour analysis – RAC

Points starting the operation of the algorithm – RAC are chosen at random in the preliminary period (Koprowski & Wróbel, 2009). Next, the correction of their number is performed, so that the remaining ones, granting proper conditions become the first points for the appointed RPE, IS/OS, NFL or OPL layers. This line become stretched further by method of modified active contour introduced in description of CCA algorithm (Fig. 14).
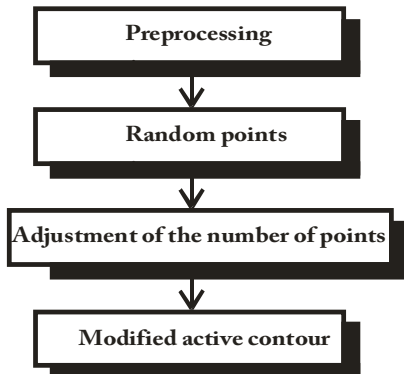

Fig. 14. Block scheme of RAC algorithm

It has already been mentioned that preliminary position of starting points was chosen at random. random values from monotonous partition were acquired (0,1) for each of new points of image matrixes - Lo (about resolution of L_{MED} image there is.: M×N). For Lo image pixels created this way (random) binarization with threshold pr is carried out . Each new pixel with value "1" will be further starting point $o*_{i,j}$ (where index "i" means next starting point however, "j" means next points created on its base). This way, by selecting value of threshold pr in range (0.1) we influence the number of starting points. In the next period, the position of starting points is modified in the assigned H area of the sizes $M_H \times N_H$. The

modification relies on correction of point position $o^*_{i,1}$ with coordinates $(x^*_{i,1}, y^*_{i,1})$ to new coordinates $(x_{i,1}, y_{i,1})$ where possibly relocation is in range $x_{i,1}= x^*_{i,1} \pm (N_H)/2$ and $y_{i,1}= y^*_{i,1} \pm (M_H)/2$. Change of coordinates follows in area $\pm (M_H)/2$ and $\pm (N_H)/2$ in which the biggest value is achieved in remainder between pixels in eight- neighbor match. Next the correction of repeating points is performed- this which have the same coordinates are deleted.

For assigning layers on OCT image the component of contour were later indicated in meaning of his fragments subjected later to modification and processing in the following manner. For each $o^*_{i,1}$ point chosen at random with coordinates $(x^*_{i,1}, y^*_{i,1})$ iteration process is performed relying on searching of next $o_{i,2}$, $o_{i,3}$, $o_{i,4}$, $o_{i,5}$ points and so on, according to dependence described in CCA algorithm (Fig. 8).

In the described case of iteration appointment contour component becomes essential introduction of limitation range (next parameters) which includes:

- j_{MAX} - maximum number of iterations - limitation whose purpose is to eliminate algorithm looping if every time, points $o_{i,j}$ will be appointed with different locations and contour will have for example spiral form.
- Stopping the iteration process if it will be discovered that $x_{i,j}=x_{i,j+1}$ and $y_{i,j}=y_{i,j+1}$. This situation happens most often if Lu and Ld areas are of a similar size as area H or are bigger (about sizes $M_H \times N_H$). As for the random choosing and correcting starting points, here might also appear the situation that after the correction there will be $x_{i,j}=x_{i,j+1}$ and $y_{i,j}=y_{i,j+1}$
- Stopping the iteration process if $y_{i,j}>M_M$ or $x_{i,j}>N_M$ or in cases where the indicated $o_{i,j}$ point will be outside the picture.
- Stopping the iteration process if still better matching point in respect does not grant condition admissible $\Delta\alpha$ (allowable curvature contour).

At this stage, components of the outline for the given parameters are obtained. These parameters include:

Size of h_x and h_y mask is strictly related to resolution of image and size of identified area accepted for $M_M \times N_M = 864 \times 1024$ on $M_H \times N_H = 23 \times 23$

p_r – threshold responsible for the number of starting points - changed practically in range 0-0.1,

j_{MAX} - maximum admissible number of iterations - established arbitrarily at 100,

$\Delta\alpha$ - partition of angle established in partition 10-70°,

$M_H \times N_H$ -size of correction area, square area, converted in range $M_H \times N_H=5 \times 5$ to $M_H \times N_H=25 \times 25$

$\Delta\alpha$ – admissible maximum change of angle between the folowing points of contour established in partition 10-70°.

The analyzing the acquired values it must be noticed that stopping the iteration process happens only when $x_{i,j}=x_{i,j+1}$ and $y_{i,j}=y_{i,j+1}$ (as it was said earlier). Or then only if points $o_{i,j}$ and $o_{i,j+1}$ have the same position. This condition does not concern oi,j points which have the same coordinates but for different "i", that is the ones that emerged in definite point of iterations from different initial points. Easing of this condition leads to generation overlap on the elements of contour which must be analyzed.

As it has been presented above, the performed iteration process can cause overlapping of $o_{i,j}$ points with the same coordinates $(x_{i,j}, y_{i,j})$ emerged from different initial $oi,1$points. This property is used for ultimate appointment of contour layers on OCT image.

In a general case, it can happen that despite relatively small values of the accepted p_r threshold, the randomly chosen $o_{i,1}$ starting point is placed beyond the edge of object. Then, the next iterations can join it with the remaining part. In such a case the deletion process of outstanding branch is performed – alike for lopping off of branch in frameworking (Gonzalez & Woods, 1992).

Exemplary results showed on Fig. 15 are acquired for real OCT image for $p_r=0.02$, $\Delta\alpha=80^o$, $M_H \times N_H = 35 \times 35$.
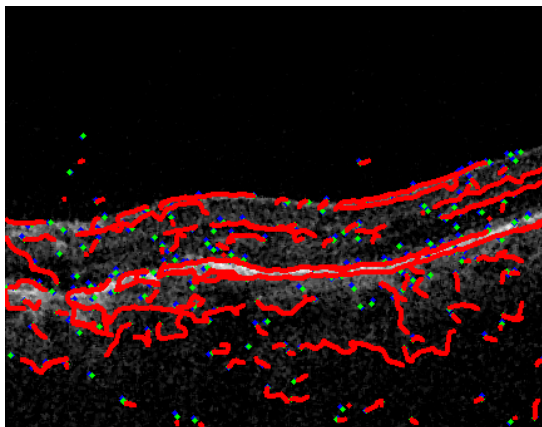
Fig. 15. Exemplary results acquired for real image OCT for $p_r=0.02$, $\Delta\alpha=80^o$, $M_H \times N_H = 35 \times 35$.

Fig. 1 - correctly indicated contour components are visible and other fragments of contour which from the point of view of limitation are not deleted. However, on the other hand number of available parameters and its form allow enough liberty in their selection in order to get desired results. In majority of cases, obtaining the intentional form of contour is possible for one established $M_H \times N_H$ value. However, it can turn out that the use of hierarchic approach is required for which $M_H \times N_H$ size will be decreased, thanks to which greater accuracy of the suggested method will be acquired and it will introduce weight (hierarchies) of importance of individual contours.

3.5 Method based on hierarchic approach – HAC

The method based on hierarchic approach – HAC (Koprowski & Wróbel, 2009).The main NFL or RPE layers are initially identified on image of the smallest resolutions and next remaining layers are identified like for example IS/OS and accuracy reconnaissance of NFL and RPE layers (Fig. 3-2) is gradually increased.

From foundation, described algorithm should give satisfactory results mainly from part of criterion operation speed. The described methods (algorithms) are characterized by big accuracy of account, however, they are not sufficiently fast (it is hard to get analysis speed of single 2D image in time not surpassing 10ms or 50 ms on processor PII 1.33 GHz). Thus, decrease of L_{MED} image resolution was suggested about near 50% for such value of pixels number in rows and columns (with $M \times N=740 \times 800$) which is power of value "2" there is $M \times N=256 \times 512$ (L_{MED2}) applying further decomposition for L_{D16} image (where symbol "D" – means decomposition and symbol "16" means block size for which it has been received). Any exit (output) image pixel after decomposition has value equal median from area (block) of 16×16 size entrance (input) image according to Fig. 17.
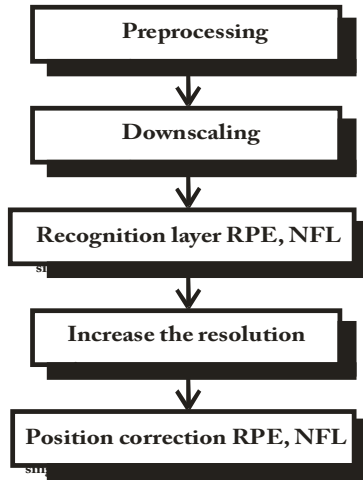
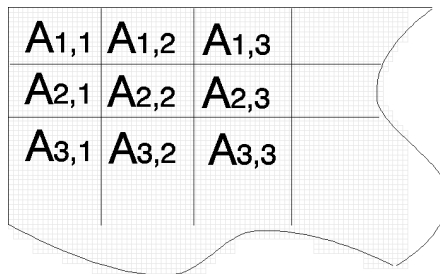Fig. 16. Block scheme of HAC algorithm
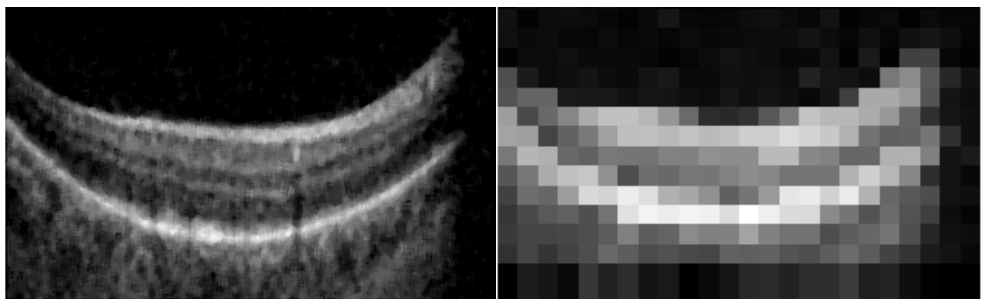

Fig. 17. Location of blocks na obrazie L_{MED2}

Fig. 18. Image before and after decomposition – L_{MED2} i L_{D16}

Exemplary L_{D16} result and input L_{MED2} image are shown on Fig. 18. L_{D16} Image will be subjected to the operation of appointment of pixel positions with maximum value for each column. Applying this thresholding method by maximum value in rows, in 99% of cases only one maximum value in column is received.

Fig. 19. Exemplary L_{DB16} image

In order to appoint position of NFL and RPE borders precisely, the use one more L_{DB16} image was essential. This image is a binary image with white pixels placed in places for which remainder between neighbor pixels in vertical tis greater than assigned pr threshold – accepted in range (0, 0.2). In result, the cooridnates of points border locations $y_{NFL}^{(HAC)}$ and $y_{RPE}^{(HAC)}$ are received as locations of values "1" in L_{DB16} image for which $y_{NFL}^{(HAC)}(x) \leq y_{RPE}^{(HAC)}(x)$. This relative simple approach gives unbelieveably satisfactory results. This method for selection of pr threshold on level 0.01 gives satisfactory results in nearly 70% of images in not compound cases (that is, the ones which are not images with visible pathology or shield of optical nerve). Unfortunately, for the remaining 30% of cases, selection of p_r threshold in accepted borders does not decrease the emerging errors (Fig. 19).

The correction of erroneous reconnaissance of $y_{NFL}^{(HAC)}$ and $y_{RPE}^{(HAC)}$ layers is important because for this approach these errors will be copied (In presented further hierarchic approach) for next exact approximations. After correction taking into consideration number of white pixels for individual L_{DM16} image columns, and mutual situating taking into consideration NFL and RPE layers position, presented correction gives for above-mentioned images class efficiency at the level of 99% of cases. Despite the accepted limitations, this method brings erroneous results for initial columns of image (with hierarchic approach definition) unfortunately, these errors are copied further.

The cause of erroneous reconnaissance of layers locations is the difficulty in distinguishing proper layers in case of discovering three "line", three points in given column in which position is changed in admissible range for individual x.

3.6 Decrease of decomposition area

Relatively simple period of processing of tomographyc image with particular consideration of speed of operation is escalation of accuracy and the same decrease of $A_{m,n}$ area's size (Fig. 17) – block on L_{MED} image. It was assumed that $A_{m,n}$ areas will be decreased in sequence to 1×1 size by a half in each iteration. Decrease of $A_{m,n}$ area is equivalent with next period execution of NFL and RPE line position approximation.

Increase of accuracy (precision) position of NFL and RPE lines indicated in former iteration is tied with two periods:

- Coordinate condensing (x,y) in meaning of indirect appointment (in center of point (x,y) put exactly) using method of linear interpolation.
- Change of position of the condensed points so that they bring closer the wanted borders in a better way.

If first part is intuitive and it leads to resampling process, the second requires exact explanations.The second period relies on adjusting individual point to wanted layer. Because in ox axis the image is from definition already decomposed and pixel brightness in the analyzed image is similar to median value of the primary image, properly in window A (Fig.17) modification of RPE and NFL point position follows in vertical axis only. Analysis of individual RPE and NFL points is independent in meaning of addiction from the position of point in line.
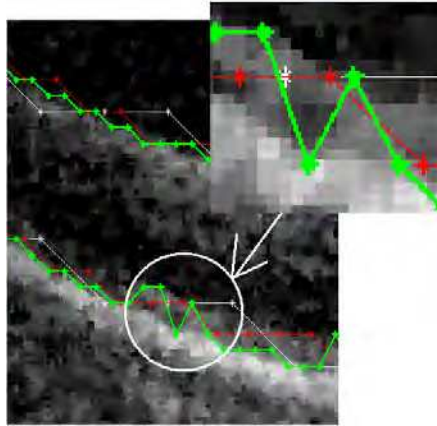
Fig. 20. Results of the processes of adjusting for two iterations. White color marks input RPE points and red and green color mark next approximations.

Each RPE point remaining from the previous iteration and new arising from the interpolation, are in various stages of the algorithm matched to RPE layer with ever greater precision. Change of the position of $y_{RPE}^{(HAC)}$ point (x) is in the range $\pm p_u$ where range of variation is not dependent on the scale of considerations (size of A area) and follows closely the distance between the NFL and RPE. For blocks A of size 16×16 to 1×1 p_u is constant and is 2. This value was adopted on the basis of the typical average for examined hundreds of L_{GRAY} images the distance between the NFL and RPE of about 32 pixels which means that the decomposition into A blocks of size 16×16 are two pixels so $p_u = 2$. In this regard, ± 2 is looking for maximum L_{DM} image and it adopts a new position of RPE NFL point. This way the process of RPE or NFL is more similar to the actual conduct of the analyzed layer. Results obtained from the fit shown in Fig. 3-6. The white color shows the input RPE values as input data for this stage of the algorithm and the decomposition on A blocks of size 16×16 (L_{DM16} and L_{D16} images), red matching results for A blocks of size 8×8 (L_{DM8} and L_{D8} images) and green match results for A blocks of size 4×4 (L_{DM4} and L_{D4} images). As shown in Fig. 3-6 further decomposition and the next smaller and smaller A areas and hence higher resolution, image is obtained with greater accuracy at the expense of time (Indeed, increasing the number of analyzed $y_{RPE}^{(HAC)}(x)$, $y_{NFL}^{(HAC)}(x)$ points and their neighborhoods $\pm p_u$).

This method for A size 16×16 has large enough properties of the Global Approach to the brightness of pixels that there is no need to introduce at this stage the additional treatment to distinguish between closely spaced layers (that were not previously visible because of image resolutions). By contrast, with the A areas of sizes 4×4 other layers are already

visible, which should be further analyzed correctly. Increasing accuracy makes IS/OS layer visible which is located near the RPE layer (Fig. 20). Thus, in a circled area there is high fluctuation of position in oy axis of RPE layer. Therefore, a next algorithm step was developed taking into account the partition on RPE and IS/OS layers for appropriate high-resolution. As shown in Fig. 21. presented method copes perfectly with detection of NFL, RPE and IS/OS layers marked appropriately by colors red, blue and green.
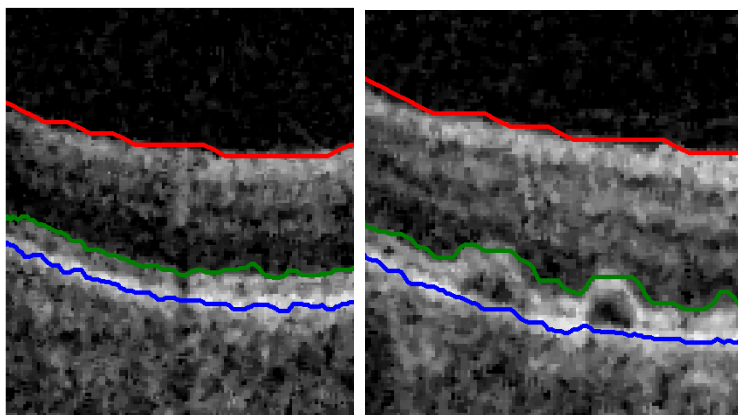
Fig. 21. Fragments of L_{MED} images with drawn NFL course– red, RPE – blue and IS/OS – green

4. Summary

Presented methods ACM, CCA, RAC or HAC give correct results at detection (identifying) RPE, IS/OS, NFL or OPL layers on tomographyc image of eye. Differences in suggested methods are visible only at their comparison of efficiencie for analysis of some hundreds mentioned tomographyc images. Comparing the mentioned methods we must bear in mind accuracy of reconnaissance of layer, reactions of algorithms on pathologies, shields of optical nerves and speed of operation in this case for computer (P4 CPU 3GHz, 2GB RAM).

The following table Tab 1 shows composite comparison of the suggested algorithms and Tab. 2. comparison of result acquired with assistance of the discussed algorithm taking into consideration typical and critical fragments of operations of individual algorithms.

Algorithm/Feature	ACM	CCA	RAC	HAC
Total error in the diagnosis of layers	5%	4%	7%	2%
The rate of detection layer RPE - MATLAB	15 s	5s	10s	1s
The rate of detection layer RPE - C++	0.85 s	0.27s	1.2s	50ms

Table 1. Composite comparison of the suggested algorithms

Random. Described method gives correct results at appointment of contour (separation of layers) equal on OCT images and for other images for which classic methods of appointment of contour they not bring results or results do not supply continuous contour. Big influence of hum on the acquired results is one of the algorithm's defects. It results from

fact that number of pixels with big value that is the disturbance increases the possibility of choosing at random the starting point in this place and in consequence element contour. Time of account is the second defect which is greater if the number of chosen points is greater /or cause for which next $o_{i,j+1}$ points search has been detained.
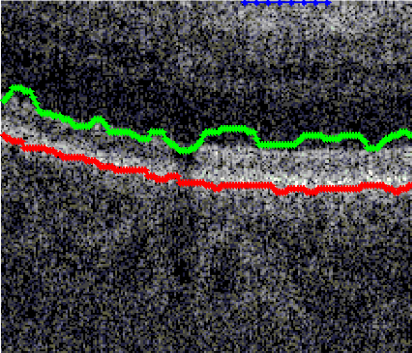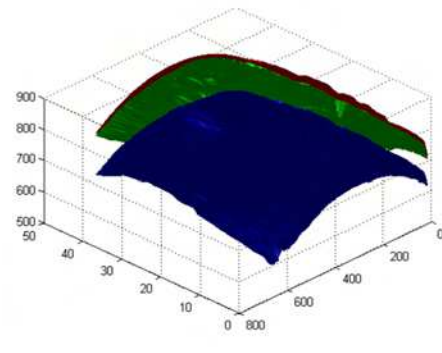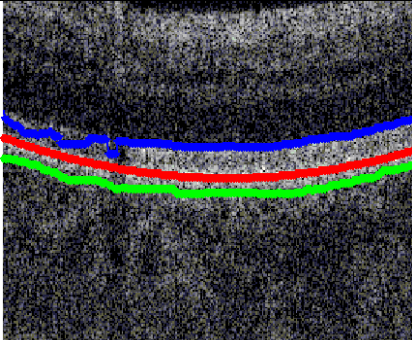
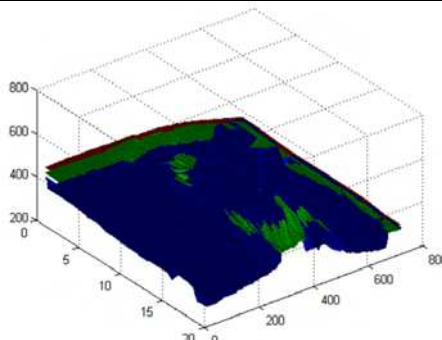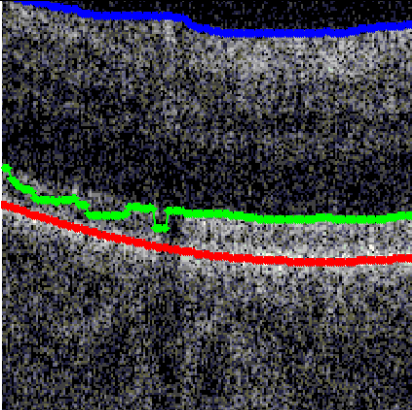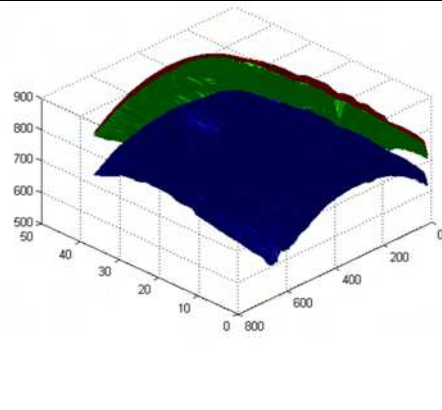| Method	A case of wrong diagnosis - due to the nature of the method	Sample reconstruction of 3D NFL layers - blue, RPE - red and IS / OS – green
ACM		
CCA		
RAC		

Table 2. Comparison of the results obtained by the described algorithms

Hierarhic. Presented algorithm discovers NFL, RPE and IS/OS layers in time for 50ms on computer with processor 2.5GHz Intel Core 2 Quad. Performed measurement of time was measured as value of average analysis 700 images dividing individual images on A blocks (Fig. 3-3) about sizes 16×16, 8×8, 4×4, 2×2. It is possible to decrease this time by modifying number of approximation blocks and simultaneously boosting identification error of position of layer - results shown in a table below.

Summary of the various stages of analysis time algorithm presented in the table above clearly indicates that the first phase of the longest pre – stage processing image where the dominant importance (in terms of execution time) has a filtration of median filter and the final stage of determining the exact location of the RPE and IS/OS layers. The exact breakdown of RPE and IS / OS, in fact involves an analysis of and the correction of the position of credits primarily RPE and IS / OS in all columns for the most accurate image zoom (due to the small distance between the RPE and IS / OS is not possible to carry out this division in the previous approximations). The reduction in computation time can therefore occur only by increasing the layer thickness of measurement error. And so, for example, for analysis in the first approximation for a size 32 × 32 and then 16 × 16 thick errors arising in the first stage and reproduced in subsequent. For the approximations for A of size 16 × 16 and then 8×8, 4×4, 2×2 and 1×1 the highest accuracy is achieved but the calculation time increases approximately twice.

A key element that crowns the results obtained from the proposed algorithm is a 3D reconstruction based on the sequence of $L_M(i)$ images. The sequence of images and more precisely the location sequence of $NFL^{(i)}(n)$, $RPE^{(i)}(n)$ and $IS/OS^{(i)}(n)$ layers based 3D reconstruction tompgraphyc image. For example a sequence of 50 images and the resolution of one $L_M(i)$ image on level M×N=256×512 is obtained through the 3D image composed of three layers of the NFL, RPE and IS/OS of size 50 × 512. The results shown in (Koprowski & Wróbel, 2008),for example the reconstruction of the original image (without the treatment described above) based on the pixel brightness - reconstruction performed using the algorithm described above based on the $NFL_{(i)}(n)$, $RPE^{(i)}(n)$ and $IS/OS^{(i)}(n)$ information.
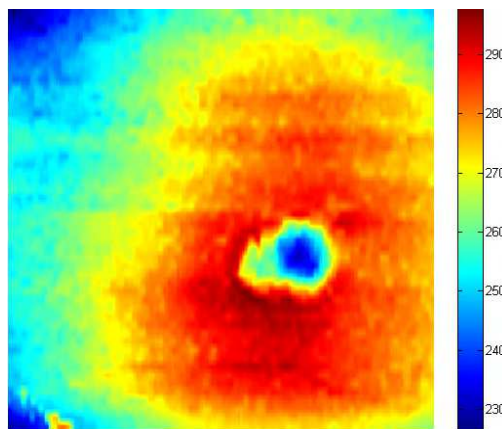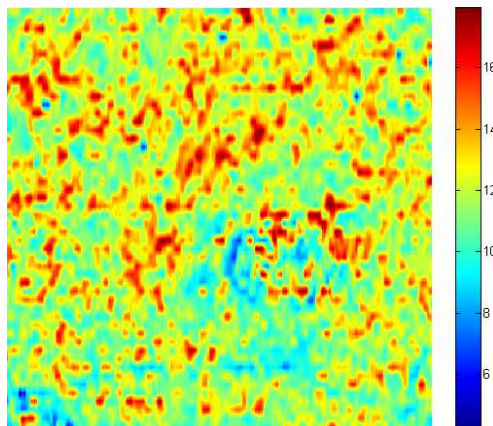

Fig. 22. Spatial location layers RPE

Fig. 23. Layer thickness IS/OS-RPE

It is clearly apparent from the layers of the ability to automatically determine locations of thickest positions or the thinnest between any points.

5. References

Adler D. C., Ko T. H., & Fujimoto J. G., "Speckle reduction in optical coherence tomography images by use of a spatially adaptive wavelet filter," Opt. Lett. 29, 2878–2880 (2004).

Akiba, M., Chan, K. P. & Tanno, N., Full-field optical coherence tomography by twodimensional heterodyne detection with a pair of CCD cameras. Optics Letters, 2003. 28(10): p. 816-18.

Barry C.: Optical Ccoherence tomography for retinal imaging dissertation, De promotor: Prof. Dr. T.G. van Leeuwen, De copromotor: Prof. Dr. J.F. de Boer 2005

Bauma B. E. & Tearney G. J.: Handbook of Opticall Coherence Thomography, MarcelDekker 2002

Canny J.: A Computational Approach to Edge Detection, IEEE Transactions on Pattern Analysis and Machine Intelligence, Vol. 8, No. 6, Nov. 1986.

Chinn, S. R. & Swanson, E. A. e Fujimoto, J. G., Optical coherence tomography using a frequency-tunable optical source. Optics Letters, 1997. 22(5): p. 340-342.

Choma MA, Sarunic MV, Yang C & Izatt JA. Sensitivity advantage of swept source and Fourier domain optical coherence tomography. Opt Express 2003 11:2183–9.

Costa, R. A., Skaf, M., et al., Retinal assessment using optical coherence tomography. Progress in Retinal and Eye Research, 2006. 25(3): p. 325-353.

Drexler W, Sattmann H, Hermann B, et al. Enhanced visualization of macular pathology with the use of ultrahigh-resolution optical coherence tomography. Arch Ophthalmol 2003;121:695–706. [PubMed: 12742848]

Farsiu S, Chiu SJ, Izatt JA. & Toth CA. Fast detection and segmentation of drusen in retinal optical coherence tomography images. Proceedings of Photonics West, San Jose, CA, February 2008; 68440D1-12 and Proc. SPIE, Vol. 6844, 68440D (2008);

Fercher AF, Hitzenberger CK, Kamp G. & Elzaiat SY. Measurement of intraocular distances by backscattering spectral interferometry. Opt Commun 1995;117:43–8.

Gnanadurai D. & Sadasivam V., "Undecimated wavelet based speckle reduction for SAR images," Pattern Recognition Letters, 26, 793-800 (2005).

Gonzalez R. & Woods R.: Digital Image Processing, Addison-Wesley Publishing Company, 1992, Chap. 4.

Hausler G. & Lindner MW. Coherence radar and spectral radar-new tools for dermatological diagnosis. J Biomed Opt 1998;3:21–31.

Klinder T., Ostermann J., Ehm M., Franz A., Kneser R. & Lorenz C., Automated model-based vertebra detection, identification, and segmentation, Medical Image Analysis 13 (2009) 471–482

Ko, T. H., Fujimoto, J. G., et al., Comparison of ultrahigh- and standard-resolution optical coherence tomography for imaging macular pathology. Ophthalmology, 2005. 112(11): p. 1922-1935.

Koprowski R., Izdebska-Straszak G., Wróbel Z. & Adamek B. The cell structures segmentation with using of decision trees. Pattern Recognition and Image Analysis, Vol. 15, No. 3, 2005,

Koprowski R. & Wróbel Z.: Hierarchic Approach in the Analysis of Tomographic Eye ImageAdvances in Soft Computing, Springer Berlin / Heidelberg Volume 57, 2009, p 463-470

Koprowski R. & Wróbel Z.: Identyfication of layers in a tomographic image of an eye based on the Canny edge detection, Conference on Information Technologies in Biomedicine, 2008

Koprowski R. & Wróbel Z.: Layers Recognition in Tomographic Eye Image Based on Random Contour Analysis Advances in Soft Computing, Springer Berlin / Heidelberg Volume 57, 2009, p 471-478

Koprowski R., Wróbel Z.: Determining correspondence in stereovision images of patients with faulty posture Congress on Image and Signal Processing, 2008

Leitgeb, R. A., Drexler, W., et al., Ultrahigh resolution Fourier domain optical coherence tomography. Optics Express, 2004. 12(10): p. 2156-2165.

Liang J, McInerney T. & Terzopoulos D.:United Snakes, Medical Image Analysis, Volume 10, Issue 2, April 2006, Pages 215-233

Ozcan A., Bilenca A., Desjardins A. E., B. E. Bouma B. E., & Tearney G. J., "Speckle reduction in optical coherence tomography images using digital filtering," J. Opt. Soc. Am. A. 24, 1901-1910 (2007).

Thrane L.: Optical Coherence Tomography: Modeling and Applications, Risø National Laboratory, Roskilde, Denmark, May 2001
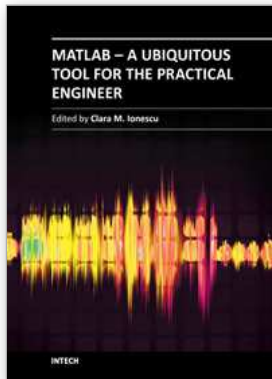
MATLAB - A Ubiquitous Tool for the Practical Engineer

Edited by Prof. Clara Ionescu

A well-known statement says that the PID controller is the â€œbread and butterâ€ of the control engineer. This is indeed true, from a scientific standpoint. However, nowadays, in the era of computer science, when the paper and pencil have been replaced by the keyboard and the display of computers, one may equally say that MATLAB is the â€œbreadâ€ in the above statement. MATLAB has became a de facto tool for the modern system engineer. This book is written for both engineering students, as well as for practicing engineers. The wide range of applications in which MATLAB is the working framework, shows that it is a powerful, comprehensive and easy-to-use environment for performing technical computations. The book includes various excellent applications in which MATLAB is employed: from pure algebraic computations to data acquisition in real-life experiments, from control strategies to image processing algorithms, from graphical user interface design for educational purposes to Simulink embedded systems.

How to reference

In order to correctly reference this scholarly work, feel free to copy and paste the following:

Robert Koprowski and Zygmunt Wróbel (2011). Selected Methods of Image Analysis in Optical Coherence Tomography, MATLAB - A Ubiquitous Tool for the Practical Engineer, Prof. Clara Ionescu (Ed.), ISBN: 978-953-307-907-3, InTech, Available from: http://www.intechopen.com/books/matlab-a-ubiquitous-tool-for-the-practical-engineer/selected-methods-of-image-analysis-in-optical-coherence-tomography

INTECH
open science | open minds